Brain Research 1677 (2017) 14–19

Contents lists available at ScienceDirect

Brain Research

journal homepage: www.elsevier.com/locate/bres

Research report

Hippocampal metabolism and prefrontal brain structure: A combined 1H-MR spectroscopy, neuropsychological, and voxel-based morphometry (VBM) study

Johanna Steinke [a], Christian Gaser [a,b], Kerstin Langbein [a], Maren Dietzek [a], Alexander Gussew [c], Jürgen R. Reichenbach [c], Stefan Smesny [a], Heinrich Sauer [a], Igor Nenadić [a,d,*]

[a] Department of Psychiatry and Psychotherapy, Jena University Hospital, Jena, Germany
[b] Department of Neurology, Jena University Hospital, Jena, Germany
[c] Medical Physics Group, Institute for Diagnostic and Interventional Radiology (IDIR), Jena University Hospital, Jena, Germany
[d] Department of Psychiatry and Psychotherapy, Philipps University Marburg & Marburg University Hospital/UKGM, Marburg, Germany

ARTICLE INFO

Article history:
Received 17 April 2017
Received in revised form 9 August 2017
Accepted 1 September 2017
Available online 9 September 2017

Keywords:
Hippocampus
Magnetic resonance spectroscopy (MRS)
Voxel-based morphometry (VBM)

ABSTRACT

Hippocampal structural and functional integrity impacts on multiple remote areas of the brain, and this connectivity is central to multiple cognitive functions in healthy and disease. We studied associations of hippocampal metabolic markers N-acetyl aspartate (NAA) and glutamate (Glu and Glx; assessed with 1H magnetic resonance spectroscopy) and brain grey matter (studied with voxel-based morphometry, VBM) in 20 healthy subjects. We found a significant correlation between right hippocampal NAA and left ventrolateral prefrontal cortical grey matter (TFCE, $p < 0.05$, FWE-corrected), as well as verbal fluency markers, and right hippocampal Glx (glutamate/glutamine) and left cerebellar volume. Our studies demonstrate a structure-function correlation that might underlie the interaction of the hippocampus with prefrontal cortex and cerebellum, which might be central to several neurological and psychiatric disorders, including schizophrenia or depression.

1. Introduction

Hippocampal integrity is central to a number of cognitive and emotional functions. Alteration of hippocampal structure and/or function is thus also crucial for a number of pathologies, including mesial sclerosis in epilepsy (Brazdil et al., 2009), but also in depression and schizophrenia (de Diego-Adelino et al., 2013; Kraguljac et al., 2013; Nenadic et al., 2015), post-traumatic stress disorder (O'Doherty et al., 2017), as well as Alzheimer's disease (Wang et al., 2015).

The connectivity of the hippocampus with other brain structures, especially prefrontal cortices, has been a focus of recent research aiming at providing a better understanding of its role in disease (Li et al., 2015; Sigurdsson and Duvarci, 2015). Indeed, the hippocampus shows intricate connections not only to other adjacent medial temporal lobe brain structures, but also features prominent functionally relevant connections to the thalamus (Tsanov and O'Mara, 2015) and prefrontal cortex (Godsil et al., 2013).

Multi-modal imaging is an approach to study such interactions, combining different MR modalities to assess structure and/or function. Examples of this are recent studies, which have linked hippocampal structure and metabolism in epilepsy (Brazdil et al., 2009) and schizophrenia (Hasan et al., 2014; Kraguljac et al., 2013), respectively. In the present study, we used MR spectroscopy (MRS) in healthy subjects to assess hippocampal metabolite levels for N-acetyl aspartate (NAA) as a marker of neuronal viability and glutamate (Glu) (assessed as Glu and Glx), and to correlate those with grey matter structural variation across the brain.

2. Results

Quantitative metabolite levels are given in Table 1.

Right hippocampus NAA concentration correlated significantly with a cluster in the left ventrolateral prefrontal cortex (PFC) at $p < 0.05$ FWE-corrected ($k = 93$ voxels; maximum voxel at −38; 32; −8). Right hippocampus Glx (glutamate and glutamine combined) correlated significantly ($p < 0.05$, FWE-corrected) with two clusters in the left lateral cerebellum ($k = 1984$ voxels, maximum

* Corresponding author at: Department of Psychiatry and Psychotherapy, Philipps University Marburg & Marburg University Hospital/UKGM, Rudolf-Bultmann-Str. 8, 35037 Marburg, Germany.
E-mail address: nenadic@staff.uni-marburg.de (I. Nenadić).

https://doi.org/10.1016/j.brainres.2017.09.004
0006-8993/

Table 1
Quantitative levels of metabolites (mean and SD).

Metabolite level (mmol/l)	Left hippocampus mean (SD)	Right hippocampus mean (SD)
N-acetyl aspartate (NAA)	8,89 (2,88)	9,46 (3,03)
Glutamate (Glu)	9,07 (3,14)	9,87 (2,53)
GLX (glutamate + glutamine)	13,73 (5,16)	16,12 (4,46)

at −40; −55; −48; and k = 333, maximum at −45; −78; −27), but this was not significant in the glutamate correlation analysis. Results are shown in Fig. 3.

While there were no other significant correlations at corrected thresholds, we did find additional correlations in an exploratory analysis ($p < 0.001$, uncorrected): 1.) For right hippocampal NAA, we found additional positive correlations in the left dorsolateral PFC, right medial PFC, left anterior insula/capsula extrema grey matter, right central sulcus grey matter, and a minor cluster in the right dorsolateral PFC. 2.) For left hippocampal NAA, we found positive correlations in a left orbitofrontal/ventrolateral PFC cluster, left medial PFC, and right central sulcus grey matter, as well as a negative correlation with a small right parietal cluster; or right hippocampal glutamate, we found positive correlations in a left ventrolateral PFC cluster, right medial PFC, right dorsolateral PFC, as well as negative correlation with left amygdala and left posterior cerebellum; for left hippocampal glutamate, we found positive correlations in clusters in the left anterior temporal pole and a smaller cluster in the right medial parietal cortex/precuneus, right middle temporal gyrus, and a negative correlation in a small right caudate cluster. 3.) For right hippocampal Glx, we there was no additional correlation (apart from the two cerebellar clusters significant at corrected thresholds). 4.) Finally, for left hippocampal Glx, there was a negative correlation with the right caudate and a positive with right precuneus, right middle temporal gyrus, and left middle occipital cortex.

Overall, we did not find either positive or negative correlations of hippocampal metabolic parameters with hippocampal grey matter.

Correlation analyses with neuropsychological data showed a significant positive correlation ($p < 0.05$) of right hippocampal NAA with COWT-S ($r = 0.4$, $p = 0.04$). Information score (from WIE/WAIS) showed negative correlations with left hippocampal NAA ($r = -0.49$; $p = 0.02$) and left hippocampal Glx peaks ($r = -0.53$; $p = 0.01$).

3. Discussion

This study demonstrates an association of hippocampal metabolic markers with prefrontal cortex and cerebellar brain structure. Using a multi-modal approach, these findings serve to understand the inter-relations of brain functional and structural interactions. We used NAA and Glx as these are the most studied ^{1}H-MRS parameter for a range of neurological and psychiatric disorders, and have been studied in depth in previous MRS studies (for overview, see (Ramadan et al., 2013)). Three aspects from our findings merit particular attention.

First, the association of NAA, a marker of general neuronal integrity, with left ventrolateral prefrontal cortex volume suggests an interaction of these two brain structures. Their connectivity is central to memory tasks (Takita et al., 2013). This seems to be the case not only for medial PFC regions; recent meta-analyses suggest ventrolateral PFC and medial temporal lobe activation particularly during encoding of episodic memory (Spaniol et al., 2009). Given that our study combines MRS and VBM, it differs from purely functional techniques assessing connectivity, such as analyses of functional connectivity based on fMRI. MRS rather directly captures aspects of metabolites and thus gives evidence additional to BOLD changes tapped in fMRI. In our study, hippocampal NAA was also related to performance on verbal fluency, which is in line with previous fMRI studies (Glikmann-Johnston et al., 2015). Notably, this prefrontal-hippocampal link has multiple implications of disturbed connectivity in psychiatric disorder (Godsil et al., 2013; Li et al., 2015).

Secondly, our glutamatergic findings link hippocampal Glx to cerebellar function. Glutamate has be linked to cognitive functions in multiple MRS studies (Ende, 2015), as it is of central interest to multiple neuropsychiatric disorders (Ramadan et al., 2013). Research on the interaction between the hippocampus and cerebellum and its implications in cognition, however, are by far more scarce. This connection has received more interest in research using fMRI and computational modelling elucidating the interaction and its importance in cognitive processing, such as timing (Yu and Krook-Magnuson, 2015); the recent functional anatomical models stress a bidirectional influence. Recent examples of the cognitive significance of this connection include timing-sensitive prediction of movements (Onuki et al., 2015) and non-motor aspects of navigation (Igloi et al., 2015). Our findings therefore provide additional structure-function evidence of an interaction.

While we only found this association with the Glx sum peak, the lack of significance with Glu might be, in part, due to methodological limitations in isolating the peak, possibly leading to increased variance (Gussew et al., 2012). Also, we need to consider that glutamatergic peaks in MRS might be related to other measures of overall metabolism (Smesny et al., 2015; Squarcina et al., 2017), reminding us of the possibility that MRS possibly not exclusively detects synaptic glutamate but also other non-vesicular forms of this metabolite.

Finally, one negative finding also merits attention: we did not find an association of hippocampal metabolic markers with hippocampal grey matter itself, as suggested by some previous work in schizophrenia (Kraguljac et al., 2013). This might, in part, be attributable to the functional heterogeneity within the hippocampus (Wagner et al., 2016). Increased spatial resolution within the hippocampus would be needed to assess this in further studies.

Our findings suggest further research in several aspects. For example, the limited sample size in our study precluded an in-depth exploration of the effects of age and gender, which have been described for brain metabolites (Jung et al., 2005; Raininko and Mattsson, 2010), but have not been studied in further detail for the association of metabolites and brain structure. While our findings are highly significant, they might only hold for a particular age range and structure-function correlations might differ in children or adolescents.

One methodological limitation of our study relies on the ambiguity of resolving the overlapping resonance patterns in the chemical shift range between 2.1 and 2.4 ppm. Despite being dominated by glutamate signals, the quantitated intensities might be particularly blurred by glutamine and GABA contributions, which might not be fully differentiated even by LCModel quantitation performed with dedicated metabolite model basis set. Therefore, we are working on implementation of more advanced quantitation methods in order to achieve more reliable separation between these metabolites in future studies (Belkić and Belkić, 2016; Belkić and Belkić, 2017).

Future studies might take into account current advances in separating MRS peaks and identify associations with brain structures. For example, separation of glutamate and glutamine as well as addition of gamma-amino-butyric acid (GABA) to such association studies will strengthen our understanding of how specific

metabolic parameters relate to underlying brain structure (Ramadan et al., 2013). This might bridge the gap to basic neuroscience studies on the cellular level, which might directly assess glutamatergic and GABAergic neurotransmission, but are limited in providing more large-scale analyses on the systems level.

In summary, our findings provide evidence of a structure-function interaction between the hippocampus and lateral prefrontal cortex, as well as cerebellum, resp., which might be of relevance to structural and functional connectivity and its role in cognition as well as disease.

4. Experimental procedure

4.1. Subjects

We included 20 healthy unrelated subjects (12 female, 8 male; mean age 27.75 yrs, SD 6.34, range 21–45 yrs) in a study protocol approved by the ethics committee of Jena University Medical School. All subjects provided written informed consent. The studied cohort does not overlap with those of a previous study in which we combined MRS and VBM in patients with schizophrenia and healthy controls (Nenadic et al., 2015), and the present sample additionally included a neuropsychological assessment, and was directed at healthy volunteers only.

All subjects were psychiatrically healthy, with no history of current or previous psychiatric conditions or treatment, no first-degree relative with psychotic disorder, no current or previous central nervous disease or (uncontrolled) general medical condition. Further exclusion criteria were history of traumatic brain injury and learning disability (estimated IQ, based on MWT-B scores, ranged from 91 to 118; mean 103.1, SD 9.5), as well as psychotropic medication. Handedness was assessed with the Edinburgh handedness inventory (EHI, (Oldfield, 1971)), showing a mean score of 78.38 (SD 30.18; range −16.67 to 100; n = 19 available data sets). The EHI, while having been noted for some shortcomings (Fazio et al., 2013), is still among the most widely used handedness inventories.

4.2. Magnetic resonance imaging and spectroscopy

Magnetic resonance images (MRI) and MR spectroscopy data were acquired on a 3 Tesla MR system (Siemens Tim Trio, Siemens, Erlangen, Germany) on two successive days (as part of a larger imaging protocol, involving structural and functional MRI and MRS). An anatomical high-resolution scan was acquired using a twelve channel phase array head coil and a T_1-weighted MPRAGE sequence (TR 2300 ms, TE 3.03 ms, a 9°, field-of-view 256 mm, resolution $1 \times 1 \times 1$ mm). Images were visually inspected to exclude image artefacts.

MRS spectra from the left and right hippocampus were obtained using a PRESS single voxel technique (TE/TR: 30/2000 ms, 512 water suppressed and 16 water non-suppressed single acquisitions, scan time per ROI: 19 min) using a double-resonance ($^1H/^{31}P$) transmit/receive volume head coil (Biomedical Rapid GmbH, Germany). The sequence allowed acquisition of spectra in the left and right hippocampus, with each of the $30 \times 10 \times 10$ mm^3 MRS voxels positioned along the axis of the hippocampus, covering most of the hippocampus (see Fig. 1 and Fig. 2 for sample spectrum). A MPRAGE sequence (same parameters as indicated above, with the $^1H/^{31}P$ head coil) was obtained immediately prior to MRS to allow for positioning of the voxels. Subsequently, these MP-RAGE data were segmented into GM, WM and CSF compartments based on the results of an automatic subcortical segmentation performed with a standardized FreeSurfer pipeline (Gussew et al., 2012). These data were when used to determine the GM, WM and CSF volume fractions within the MRS voxel, as described previously (Gussew et al., 2012).

Prior to MRS data acquisition, zero-, first- and second order shim gradients were adjusted within the voxels with an automatic B_0-field mapping technique, followed by fine-tuning manually the first-order shim gradients (x, y and z) to achieve a water linewidth below 16 Hz. Following the rf-frequency adjustment, the water-selective suppression pulses were similarly calibrated manually (vendor specific WET scheme implementation, suppressed spectral bandwidth: 80 Hz). To ensure nearly identically located PRESS volumes for the metabolites and water, the transmitter rf-frequency was shifted by −2.35 ppm relative to the water resonance during the scans with water suppression. Non-water-suppressed scans were conducted with a non-shifted transmitter rf-frequency in order to achieve volume matching of the metabolite signals (water-suppressed scan) and the water signal (non-suppressed scan).

4.3. Data preprocessing

Anatomical scans were analysed with voxel-based morphometry (VBM) using the VBM8 toolbox (C. Gaser, Jena University Hospital, Jena, Germany; http://dbm.neuro.uni-jena.de/vbm8), based on SPM8 (Statistical Parametric Mapping, Institute of Neurology, London, UK). Data underwent automated quality assurance implemented in the VBM8 toolbox. This standard function of VBM8 calculates the correlation of one segmented image to all remaining segmented images in order to estimate the sample homogeneity. The mean correlation can be finally used to detect outliers that deviate from the sample.

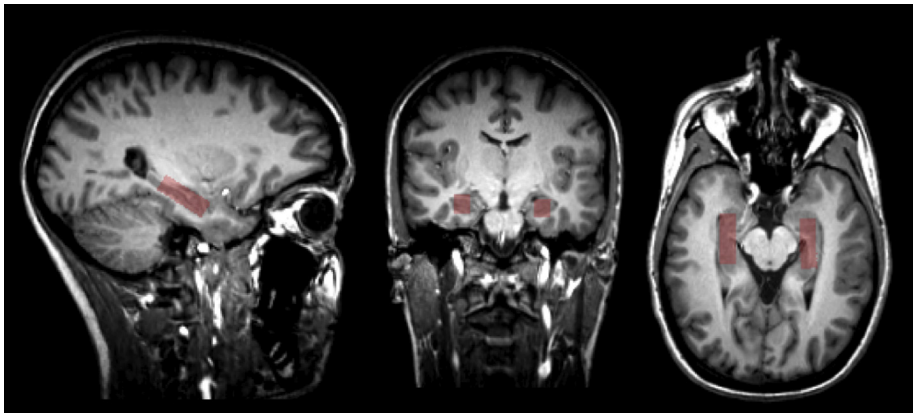

Fig. 1. Placement of hippocampal voxel for magnetic resonance spectroscopy (MRS).

Images were then normalised, segmented, and smoothed with a 12 mm full-width at half-maximum (FWHM) Gaussian kernel. We applied a more conservative absolute grey matter threshold of 0.2 to minimise artefacts on the grey/white matter borders. Grey matter images were modulated to correct for volumetric changes introduced during normalisation.

Prior to Fourier transform, the spectroscopic time signals (water-suppressed) were corrected for zero-order phase errors and eddy current distortions by using the non-suppressed water signal phase as a reference (Klose, 1990). The resulting MR spectra were then quantified with the LCModel (V 6.3., (Provencher, 1993)) by using a vendor provided basis data set with *in vitro* model spectra of 15 metabolites (NAA, creatine, glycerophosphocholine, phosphoryl-choline, glutamate, glutamine, γ-aminobutyric acid, myo-inositol, scyllo-inositol, lactate, alanine, aspartate, taurine, glucose and glycine). Metabolite intensities were fitted in the chemical shift range between 0.5 and 4.2 ppm to take into account baseline distortions caused by broad macromolecular resonances, which were also included in the model spectra basis set as simulated singlets at 0.9, 1.2, 1.4, 1.7, 2.0 and 3.0 ppm. The residual baseline course was fitted by a spline function by using the default value of LCModel hidden parameter DKNTMN (0.15). Absolute metabolite concentrations of NAA and Glu (in mmol/l) were estimated by using the intensity of non-suppressed water signal as internal reference. The T1 weighted 3D MRI brain data (MP-RAGE), which were acquired with the same head coil prior to MRS, were segmented into brain grey matter (GM), brain white matter (WM) and cerebral spinal fluid (CSF) by using a fully automatic routines included in the image analysis suite FreeSurfer (V 4.5.0, http://surfer.nmr.mgh.harvard.edu/, (Dale et al., 1999; Fischl et al., 1999)). The segmented data were then realigned with respect to the position and orientation of PRESS voxels to determine the GM, WM and CSF volume fractions in voxels (Gussew et al., 2012). The individual tissue compositions of MRS voxels were used to consider for the brain compartment specific T_1 and T_2 relaxation properties of metabolites and water as well as tissue specific water densities when calculating the absolute metabolite concentrations (Gussew et al., 2012). The relaxation correction was performed by using the *in vivo* T_1 and T_2 relaxation constants adapted from previous literature studies (see Table 2, (Choi et al., 2006; Deelchand et al., 2012; Mlynarik et al., 2001; Piechnik et al., 2009; Stanisz et al., 2005; Zaaraoui et al., 2007)). Finally, relative water densities of 0.78, 0.65 and 1 were assumed for GM, WM and CSF, respectively (Ernst et al., 1993).

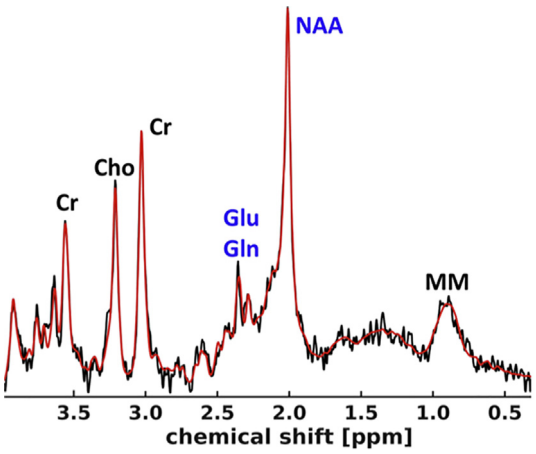

Fig. 2. Sample spectrum from magnetic resonance spectroscopy (MRS) analysis.

The MR spectra quality was evaluated by means of the NAA resonance linewidth at 2 ppm, calculated with LCModel. This information was used to detect and reject poor quality data (FWHM > 0.05 ppm). The remaining data sets that entered the analysis revealed a mean FWHM of 0.045 ± 0.007 ppm. In addition, NAA SNR was also monitored (mean: 11.2 ± 3.1). In addition, NAA SNR was also monitored (mean: 11.2 ± 3.1) as were the Cramer-Rao-Lower Bounds (SD's) for NAA and Glu intensities (mean values: SD_{NAA}: 4.7 ± 2.2 %; SD_{Glu}: 12.6 ± 4.6 %). Neither the SNR

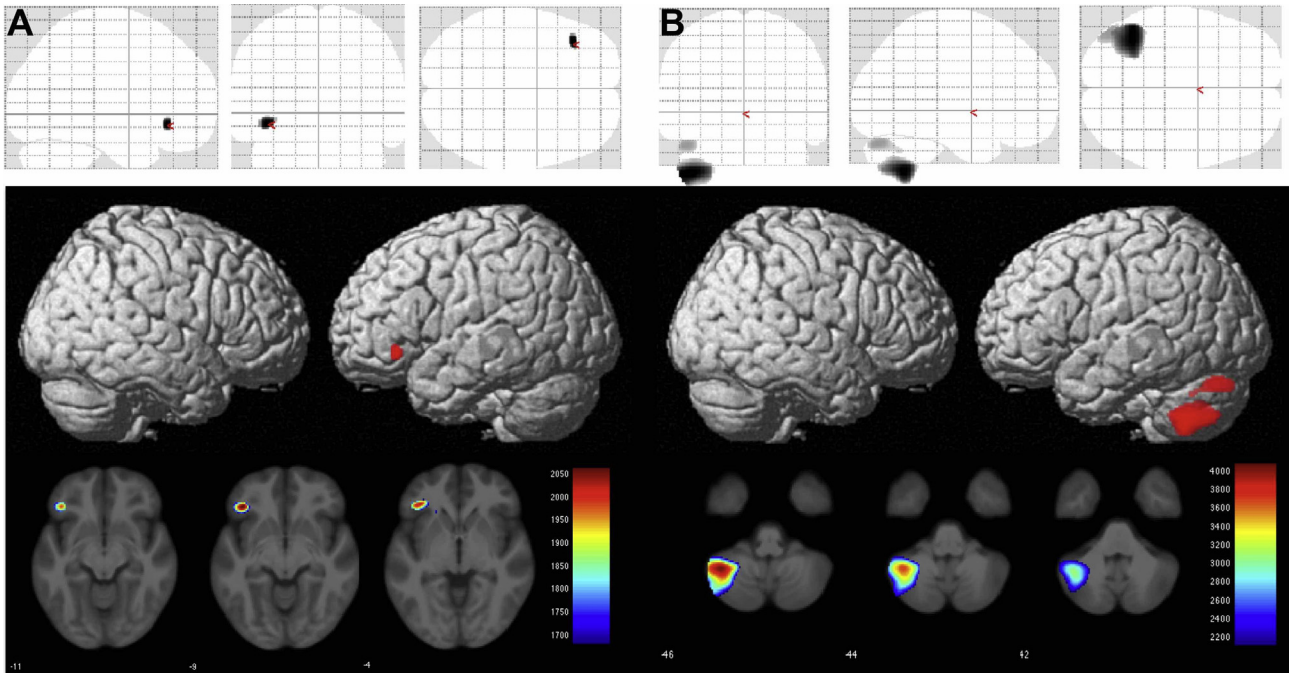

Fig. 3. Significant correlations (at $p < 0.05$, TFCE, FWE corrected; TFCE values given in colour bar) of VBM-derived grey matter values with A) right hippocampal NAA and B) right hippocampal Glx (glutamate and glutamine).

Table 2
T_1 and T_2 time constants literature values, which were used to correct the measured metabolite and water intensities for the T_2 relaxation and T_1 saturation related attenuations (Choi et al., 2006; Deelchand et al., 2012; Mlynarik et al., 2001; Piechnik et al., 2009; Stanisz et al., 2005; Zaaraoui et al., 2007).

	T_1 [s]			T_2 [s]		
	GM	WM	CSF	GM	WM	CSF
Water	1.82	1.08	3.80	0.10	0.07	0.50
NAA	1.47	1.35	~	0.21	0.19	~
Glu/Glx	1.27	1.17	~	0.16	0.17	~

nor the Cramer Rao Lower Bounds were, however, used to reject data.

4.4. Neuropsychological assessment

Subjects underwent neuropsychological assessment using the EUTwinsS battery (Goldberg et al., 2013; Toulopoulou et al., 2015), a set of cognitive tests designed to tap executive functions commonly involved in psychiatric disorders. This included six subtests from the Wechsler Memory Scale (WAIS; German version: WIE; subtests: digit-symbol-test, arithmetic, matrix reasoning, digit span, information, letter-number-sequencing), trail making test (TMT, both TMT-A and TMT-B), and the Controlled Word Association Test (COWT; in n = 19 subjects) assessing verbal fluency (with resulting variables COWT-F, COWT-A, COWT-S, and COWT-FAS).

4.5. Statistics

VBM statistical analysis was carried out using the general linear model (GLM) implemented in SPM8. Given the inter-correlation of MRS parameters, we defined four separate GLMs, each with the respective MRS parameter (left NAA, right NAA, left Glu and Glx, right Glu and Glx), as well as age and gender, for which we corrected using them as co-variates. For statistical assessment, we applied the threshold free cluster enhancement (TFCE) method (Salimi-Khorshidi et al., 2011; Smith and Nichols, 2009), and used family-wise error (FWE) correction for multiple comparisons, with a $p < 0.05$ FWE threshold.

Neuropsychological data were analysed using SPSS, performing one-tailed correlations of each neuropsychological parameter with those metabolites showing significant findings in VBM analyses (testing the hypothesis that better performance would correlate with higher metabolite levels).

Author contribution

I.N. designed the study and wrote the first draft of the manuscript.

K.L. and M.D. performed neuropsychological assessment.

K.L., M.D., St.S., H.S., and I.N. contributed to subject recruitment.

A.G. and J.R.R. contributed to MR spectroscopy analyses.

J.S., C.G., and I.N. contributed to morphometry data analysis.

Acknowledgement

Part of this study was supported by a grant of the European Union (EU) through the EUTwinsS network (European Twin Study on Schizophrenia, FP6, local PIs: I.N. and H.S.).

The authors declare that they have no other conflicts of interest.

References

Belkić, D., Belkić, K., 2016. Improving the diagnostic yield of magnetic resonance spectroscopy for pediatric brain tumors through mathematical optimization. J. Math. Chem. 54, 1461–1513.

Belkić, D., Belkić, K., 2017. Iterative averaging of spectra as a powerful way of suppressing spurious resonances in signal processing. J. Math. Chem. 55, 304–348.

Brazdil, M., Marecek, R., Fojtikova, D., Mikl, M., Kuba, R., Krupa, P., Rektor, I., 2009. Correlation study of optimized voxel-based morphometry and (1)H MRS in patients with mesial temporal lobe epilepsy and hippocampal sclerosis. Hum. Brain Mapp. 30, 1226–1235.

Choi, C., Coupland, N.J., Bhardwaj, P.P., Kalra, S., Casault, C.A., Reid, K., Allen, P.S., 2006. T2 measurement and quantification of glutamate in human brain in vivo. Magn. Reson. Med. 56, 971–977.

Dale, A.M., Fischl, B., Sereno, M.I., 1999. Cortical surface-based analysis I. Segmentation and surface reconstruction. Neuroimage 9, 179–194.

de Diego-Adelino, J., Portella, M.J., Gomez-Anson, B., Lopez-Moruelo, O., Serra-Blasco, M., Vives, Y., Puigdemont, D., Perez-Egea, R., Alvarez, E., Perez, V., 2013. Hippocampal abnormalities of glutamate/glutamine, N-acetylaspartate and choline in patients with depression are related to past illness burden. J. Psychiatry Neurosci. 38, 107–116.

Deelchand, D.K., Henry, P.G., Ugurbil, K., Marjanska, M., 2012. Measurement of transverse relaxation times of J-coupled metabolites in the human visual cortex at 4 T. Magn. Reson. Med. 67, 891–897.

Ende, G., 2015. Proton magnetic resonance spectroscopy: relevance of glutamate and GABA to neuropsychology. Neuropsychol. Rev. 25, 315–325.

Ernst, T., Kreis, R., Ross, B.D., 1993. Absolute quantitation of water and metabolites in the human brain, I. Compartments and water. J. Magn. Reson. B 102, 1–8.

Fazio, R., Dunham, K.J., Griswold, S., Denney, R.L., 2013. An Improved measure of handedness: the Fazio laterality inventory. Appl. Neuropsychol. Adult.

Fischl, B., Sereno, M.I., Dale, A.M., 1999. Cortical surface-based analysis. II: Inflation, flattening, and a surface-based coordinate system. Neuroimage 9, 195–207.

Glikmann-Johnston, Y., Oren, N., Hendler, T., Shapira-Lichter, I., 2015. Distinct functional connectivity of the hippocampus during semantic and phonemic fluency. Neuropsychologia 69, 39–49.

Godsil, B.P., Kiss, J.P., Spedding, M., Jay, T.M., 2013. The hippocampal-prefrontal pathway: the weak link in psychiatric disorders? Eur. Neuropsychopharmacol. 23, 1165–1181.

Goldberg, X., Alemany, S., Rosa, A., Picchioni, M., Nenadic, I., Owens, S.F., Rijsdijk, F., Rebollo, I., Sauer, H., Murray, R.M., Fananas, L., Toulopoulou, T., 2013. Substantial genetic link between IQ and working memory: implications for molecular genetic studies on schizophrenia. the European twin study of schizophrenia (EUTwinsS). Am. J. Med. Genet. B Neuropsychiatr. Genet. 162B, 413–418.

Gussew, A., Erdtel, M., Hiepe, P., Rzanny, R., Reichenbach, J.R., 2012. Absolute quantitation of brain metabolites with respect to heterogeneous tissue compositions in (1)H-MR spectroscopic volumes. MAGMA 25, 321–333.

Hasan, A., Wobrock, T., Falkai, P., Schneider-Axmann, T., Guse, B., Backens, M., Ecker, U.K., Heimes, J., Galea, J.M., Gruber, O., Scherk, H., 2014. Hippocampal integrity and neurocognition in first-episode schizophrenia: a multidimensional study. World J. Biol. Psychiatry 15, 188–199.

Igloi, K., Doeller, C.F., Paradis, A.L., Benchenane, K., Berthoz, A., Burgess, N., Rondi-Reig, L., 2015. Interaction between hippocampus and cerebellum crus i in sequence-based but not place-based navigation. Cereb. Cortex 25, 4146–4154.

Jung, R.E., Haier, R.J., Yeo, R.A., Rowland, L.M., Petropoulos, H., Levine, A.S., Sibbitt, W.L., Brooks, W.M., 2005. Sex differences in N-acetylaspartate correlates of general intelligence: an 1H-MRS study of normal human brain. Neuroimage 26, 965–972.

Klose, U., 1990. In vivo proton spectroscopy in presence of eddy currents. Magn. Reson. Med. 14, 26–30.

Kraguljac, N.V., White, D.M., Reid, M.A., Lahti, A.C., 2013. Increased hippocampal glutamate and volumetric deficits in unmedicated patients with schizophrenia. JAMA Psychiatry 70, 1294–1302.

Li, M., Long, C., Yang, L., 2015. Hippocampal-prefrontal circuit and disrupted functional connectivity in psychiatric and neurodegenerative disorders. Biomed. Res. Int. 2015, 810548.

Mlynarik, V., Gruber, S., Moser, E., 2001. Proton T (1) and T (2) relaxation times of human brain metabolites at 3 Tesla. NMR Biomed. 14, 325–331.

Nenadic, I., Maitra, R., Basu, S., Dietzek, M., Schonfeld, N., Lorenz, C., Gussew, A., Amminger, G.P., McGorry, P., Reichenbach, J.R., Sauer, H., Gaser, C., Smesny, S., 2015. Associations of hippocampal metabolism and regional brain grey matter in neuroleptic-naive ultra-high-risk subjects and first-episode schizophrenia. Eur. Neuropsychopharmacol. 25, 1661–1668.

O'Doherty, D.C.M., Tickell, A., Ryder, W., Chan, C., Hermens, D.F., Bennett, M.R., Lagopoulos, J., 2017. Frontal and subcortical grey matter reductions in PTSD. Psychiatry Res. 266, 1–9.

Oldfield, R.C., 1971. The assessment and analysis of handedness: the Edinburgh inventory. Neuropsychologia 9, 97–113.
Onuki, Y., Van Someren, E.J., De Zeeuw, C.I., Van der Werf, Y.D., 2015. Hippocampal-cerebellar interaction during spatio-temporal prediction. Cereb. Cortex 25, 313–321.
Piechnik, S.K., Evans, J., Bary, L.H., Wise, R.G., Jezzard, P., 2009. Functional changes in CSF volume estimated using measurement of water T2 relaxation. Magn. Reson. Med. 61, 579–586.
Raininko, R., Mattsson, P., 2010. Metabolite concentrations in supraventricular white matter from teenage to early old age: A short echo time 1H magnetic resonance spectroscopy (MRS) study. Acta Radiol. 51, 309–315.
Ramadan, S., Lin, A., Stanwell, P., 2013. Glutamate and glutamine: a review of in vivo MRS in the human brain. NMR Biomed. 26, 1630–1646.
Salimi-Khorshidi, G., Smith, S.M., Nichols, T.E., 2011. Adjusting the effect of nonstationarity in cluster-based and TFCE inference. Neuroimage 54, 2006–2019.
Sigurdsson, T., Duvarci, S., 2015. Hippocampal-prefrontal interactions in cognition, behavior and psychiatric disease. Front. Syst. Neurosci. 9, 190.
Smesny, S., Gussew, A., Biesel, N.J., Schack, S., Walther, M., Rzanny, R., Milleit, B., Gaser, C., Sobanski, T., Schultz, C.C., Amminger, P., Hipler, U.C., Sauer, H., Reichenbach, J.R., 2015. Glutamatergic dysfunction linked to energy and membrane lipid metabolism in frontal and anterior cingulate cortices of never treated first-episode schizophrenia patients. Schizophr. Res. 168, 322–329.
Smith, S.M., Nichols, T.E., 2009. Threshold-free cluster enhancement: addressing problems of smoothing, threshold dependence and localisation in cluster inference. Neuroimage 44, 83–98.
Spaniol, J., Davidson, P.S., Kim, A.S., Han, H., Moscovitch, M., Grady, C.L., 2009. Event-related fMRI studies of episodic encoding and retrieval: meta-analyses using activation likelihood estimation. Neuropsychologia 47, 1765–1779.
Squarcina, L., Stanley, J.A., Bellani, M., Altamura, C.A., Brambilla, P., 2017. A review of altered biochemistry in the anterior cingulate cortex of first-episode psychosis. Epidemiol. Psychiatr. Sci. 26, 122–128.
Stanisz, G.J., Odrobina, E.E., Pun, J., Escaravage, M., Graham, S.J., Bronskill, M.J., Henkelman, R.M., 2005. T1, T2 relaxation and magnetization transfer in tissue at 3T. Magn. Reson. Med. 54, 507–512.
Takita, M., Fujiwara, S.E., Izaki, Y., 2013. Functional structure of the intermediate and ventral hippocampo-prefrontal pathway in the prefrontal convergent system. J. Physiol. Paris 107, 441–447.
Toulopoulou, T., van Haren, N., Zhang, X., Sham, P.C., Cherny, S.S., Campbell, D.D., Picchioni, M., Murray, R., Boomsma, D.I., Pol, H.H., Brouwer, R., Schnack, H., Fananas, L., Sauer, H., Nenadic, I., Weisbrod, M., Cannon, T.D., Kahn, R.S., 2015. Reciprocal causation models of cognitive vs volumetric cerebral intermediate phenotypes for schizophrenia in a pan-European twin cohort. Mol. Psychiatry 20, 1482.
Tsanov, M., O'Mara, S.M., 2015. Decoding signal processing in thalamo-hippocampal circuitry: implications for theories of memory and spatial processing. Brain Res. 1621, 368–379.
Wagner, G., Gussew, A., Kohler, S., de la Cruz, F., Smesny, S., Reichenbach, J.R., Bar, K. J., 2016. Resting state functional connectivity of the hippocampus along the anterior-posterior axis and its association with glutamatergic metabolism. Cortex 81, 104–117.
Wang, H., Tan, L., Wang, H.F., Liu, Y., Yin, R.H., Wang, W.Y., Chang, X.L., Jiang, T., Yu, J. T., 2015. Magnetic Resonance Spectroscopy in Alzheimer's Disease: Systematic Review and Meta-Analysis. J. Alzheimers Dis. 46, 1049–1070.
Yu, W., Krook-Magnuson, E., 2015. Cognitive collaborations: bidirectional functional connectivity between the cerebellum and the hippocampus. Front. Syst. Neurosci. 9, 177.
Zaaraoui, W., Fleysher, L., Fleysher, R., Liu, S., Soher, B.J., Gonen, O., 2007. Human brain-structure resolved T(2) relaxation times of proton metabolites at 3 Tesla. Magn. Reson. Med. 57, 983–989.